Energy 218 (2021) 119364

Contents lists available at ScienceDirect

Energy

journal homepage: www.elsevier.com/locate/energy

Lambert W function based closed-form expressions of supercapacitor electrical variables in constant power applications

Joaquín F. Pedrayes*, Manuel G. Melero, Jose M. Cano, Joaquín G. Norniella, Salvador B. Duque, Carlos H. Rojas, Gonzalo A. Orcajo

University of Oviedo, Spain

ARTICLE INFO

Article history:
Received 20 December 2019
Received in revised form
11 November 2020
Accepted 15 November 2020
Available online 20 November 2020

Index Terms:
Constant power operation
Lambert W function
Supercapacitors

ABSTRACT

The traditional model used to represent the electrical behavior of supercapacitors (SCs) operating at constant power leads to a well-known differential equation which allows to obtain the charge/discharge time of the device as a function of its internal voltage. However, the opposite is not true, i.e. it is necessary to resort to numerical methods to derive the internal voltage of the SC at any specific time. In this paper, new explicit expressions for the evolution of the electrical variables involved in the charge/discharge process of a SC bank operated at constant power are derived. The proposed formulation, which is based on the use of the Lambert W function, does not only allow a straightforward calculation of all the electrical variables as a function of time, but also sheds light on the direct relations between those variables. In the assumption of validity of the classic model, the results derived in this work can be considered exact, as no further approximations are made. The accuracy of the proposal is demonstrated by comparing the results derived from the new formulation with those yielded from the classical iterative resolution of the differential equations using numerical methods. The new closed-form expressions presented in this paper have the potential to simplify the sizing, regulation and control of power applications with embedded SC banks operated at constant power.

1. Introduction

In the last years, energy storage systems are undergoing a fast development due to their innate potential of easing the growing pressure of polluting emissions on the environment. Continuous innovations in the manufacturing methods of supercapacitors (SCs) have made these devices an interesting option for the design of a wide range of energy storage applications [1]. The use of SCs are especially well-suited for processes involving abrupt power variations, as their inherent capability of dealing with high peak power values opens the door to their hybridization with other energy sources with slower dynamics [2–8]. The combination of SCs and batteries in electric vehicle charging stations serves as a good example of these type of applications [9–14]. L. Kouchachvili et al. [9] claim that the life of the batteries can be remarkably boosted by avoiding sharp current variations with the support of SC banks.

In parallel with the growing interest in the use of SCs, different models of these devices have been proposed to allow studies for the optimization of their applications. As indicated by J. F. Pedrayes et al. [15,16], this is the case of sizing SC banks or conducting an analytical characterization of their behavior. Focusing on the electrical performance, L. Zhang et al. [17] classify SC models in four different types: electrochemical, equivalent circuit, intelligent and fractional-order. From this set of alternatives, equivalent circuit models have been widely recognized due to their simplicity and accuracy in real-time energy management synthesis. In certain studies, like those conducted by P.J. Grbovic et al. [18,19] the SC is treated as a varying capacity linked to the value of its internal voltage. On the contrary, V. Musolino et al. [20] utilize more complex models in order to analyze the effect of low and high frequency currents on SC cells. A classical approach consists in assuming that the SC can be correctly represented by a series connected resistance and capacitance (RC model), with these parameters showing no correlation with the internal voltage value [21–25]. The RC model is, by far, the most widespread version used in the study of the charge/discharge process of SCs. The value of the resistance and capacitance are typically provided by manufacturers who, furthermore, add data on their dependence with temperature. In

* Corresponding author.
E-mail address: pedrayesjoaquin@uniovi.es (J.F. Pedrayes).

https://doi.org/10.1016/j.energy.2020.119364

any case, those parameters can be considered constant without significant error while in normal operating conditions, 0 to 65 °C [26,27]. Some authors like R. L. Spyker et al. [28] or O. Abdel-baqi et al. [29] use an alternative model, including a parallel resistance, which can be used to account for the leakage current; however, this is only relevant when the self-discharge phenomenon is on the focus of the analysis.

In most practical applications, SCs are operated through charge/discharge processes that take place at constant current or constant power. As it is pointed out by M.E. Fouda et al. [30], only some specific cases require a modeling of the discharge process in the contest of a constant load impedance. With the focus on constant power applications, which is the topic addressed in this work, studies as the one conducted by J. M. Miller [31], provide methods for calculating the time of a SC going from an initial specific internal voltage to a final value. However, even if this discharge time can be explicitly calculated as a function of the internal voltage, the opposite, i.e. formulating the internal voltage as a function of time in a closed-form, does not hold true. In the same context, some efforts can be found in existing literature with the aim of providing analytical expressions for other electrical values involved in the charge/discharge processes. P.J. Grbovic et al. [19,32] develop an approximate expression for calculating the discharge current and the dissipated energy as a function of time, when considering the RC series model with constant parameters. Starting from this approximate function for dissipated energy, [19] provides a method, obtained through an energy balance, to estimate the discharge time at constant power.

The present work introduces a thorough mathematical analysis which, by using the Lambert W function, accomplishes the explicit calculation of all the electrical variables involved in the charge/discharge processes of SCs operated at constant power as a function of time. Moreover, the time itself can be also explicitly calculated as a function of any of these electrical variables and, what is more, any variable involved in the process can be expressed as a function of any other electrical variable. Thus, the need to resort to numerical methods to solve the affected differential equations is completely avoided. As a consequence, the proposed formulation is potentially valuable to help in the sizing process of SC banks as well as in the design of its related controllers. The methodology used in this work resembles the one adopted by previous studies such as [33–37], in which the results yielded by the new closed-form expressions are verified by comparing them with those obtained by solving the differential equations using numerical methods.

This paper is organized according to the following structure. In section 2, an electrical analysis of the SC during a constant power discharge is conducted, yielding an expression for the time elapsed between two values of the internal voltage of the device. In section 3, the mathematical procedure, based in Lambert W function, that allows to obtain analytical expressions of all the electrical values as a function of time (or vice versa) is presented. In section 4, these expressions are applied to a case study using data from a SC cell by Maxwell Technologies. The conclusions of the paper are presented in section 5. This paper includes also an appendix to summarize the closed-form expressions derived in this contribution which may be a valuable tool for engineering practitioners and researchers working in the field.

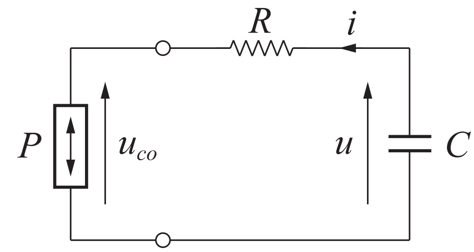

Fig. 1. Discharge of a SC at constant power.

2. Electrical analysis of SCs operated at constant power

Fig. 1 shows a SC modeled by means of its capacitance, C, and its internal resistance, R, discharging at constant power, P. The circuit also shows the discharge current, i, the internal voltage, u, and external voltage, u_{C0}, of the device.

Henceforth, in all expressions, time functions in the form $f(t)$ will be represented as f and their time derivatives as f'. The constants will be represented with capital letters. Taking into account the balance of power, it must be fulfilled that

$$P + R \cdot i^2 = u \cdot i. \tag{1}$$

In this case, the internal voltage of the SC bank can be expressed as

$$u = u_{co} + R \cdot i. \tag{2}$$

Taking into account the relationship between the current and the internal voltage of the SC when it is discharging,

$$u' = -\frac{i}{C}, \tag{3}$$

and considering (1), the following differential equation is obtained

$$R \cdot C^2 \cdot u'^2 + C \cdot u \cdot u' + P = 0. \tag{4}$$

Dividing the expression (4) by $R \cdot C^2$, then

$$u'^2 + \frac{u}{R \cdot C} \cdot u' + \frac{P}{R \cdot C^2} = 0, \tag{5}$$

where $P > 0$ for a discharge and $P < 0$ for a charge. Equation (5) has two alternative solutions. The one that leads to the lower discharge current should be chosen in order to improve the efficiency and autonomy of the SC, that is

$$u' = \frac{-u}{2 \cdot R \cdot C} + \frac{\sqrt{u^2 - 4 \cdot P \cdot R}}{2 \cdot R \cdot C}. \tag{6}$$

Thus, the time, t, needed by the internal voltage to reach each current value, u, from the initial one, U_0, can be obtain from (6) as

$$t = \frac{C}{4 \cdot P} \cdot \left[U_0^2 + U_0 \cdot \sqrt{U_0^2 - 4 \cdot P \cdot R} - u^2 - u \cdot \sqrt{u^2 - 4 \cdot P \cdot R} - 4 \cdot R \cdot P \cdot \ln\left(\frac{U_0 + \sqrt{U_0^2 - 4 \cdot P \cdot R}}{u + \sqrt{u^2 - 4 \cdot P \cdot R}} \right) \right]. \tag{7}$$

From (7), we can conclude that a closed-form expression of the internal voltage, u, as a function of time is not obvious. As a consequence, it is also not possible to derive such expression for any other electrical value related with it. Thus, in order to calculate the value of any electrical variable at a specific instant, resorting to numerical methods or approximated expressions is, up to now, mandatory. In the following section, the authors demonstrate that the use of the Lambert W function makes it possible to obtain an explicit formulation of the internal voltage, u, free of any simplification.

3. SC model formulation based on lambert W function

3.1. Lambert W function

The Lambert W function, $W(z)$, is defined as the inverse of the function $f = xe^x$ [38]; in such a way that, if $f = z$, then $W(z)$ verifies

$$W(z)e^{W(z)} = z. \quad (8)$$

Equation (8) is known as the defining expression of the Lambert W function [39] and it resembles the inverse trigonometric functions in the sense that it is a multi-valued function on a given domain. In general, z is a complex number but, in the particular case of z being real, $W(z)$ has two possible values in the interval $-1/e < z < 0$, as it can be seen in Fig. 2. The branch satisfying $W(z) > -1$ is denoted by $W_0(z)$ and it is referred as the principal branch [38]. The secondary branch, satisfying $W(z) < -1$, is denoted by $W_{-1}(z)$.

The Lambert W function was proposed to be applied in the solution of problems embracing a wide range of practical applications, such as jet fuel and combustion, models of enzyme kinetics, molecular physics, water movement in soil, epidemics and the analysis of algorithms, among others [38].

3.2. Solution based on the lambert W function

Equation (7) can be reformulated as

$$u^2 + u \cdot \sqrt{u^2 - 4 \cdot P \cdot R} - 4 \cdot R \cdot P \cdot ln\left(u + \sqrt{u^2 - 4 \cdot P \cdot R}\right) = h, \quad (9)$$

with h being a function that follows the expression

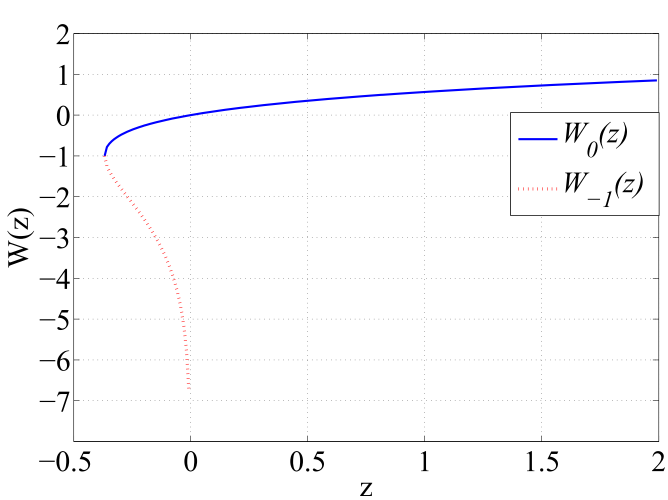

Fig. 2. Lambert W function plot showing the two real branches: $W_0[z]$ (solid line) and $W_{-1}[z]$ (dashed line).

$$h = U_0^2 + U_0 \cdot \sqrt{U_0^2 - 4 \cdot R \cdot P} - 4 \cdot R \cdot P \cdot ln\left(U_0 + \sqrt{U_0^2 - 4 \cdot R \cdot P}\right) - \frac{4 \cdot P \cdot t}{C}. \quad (10)$$

In order to clear the internal voltage from (9), a change of variable must be conducted. Thus, a new variable, z, with voltage dimensions, is defined as

$$z = -u + \sqrt{u^2 - 4 \cdot R \cdot P}. \quad (11)$$

Using (11), those terms appearing in (9) that are a function of the internal voltage, u, can now be expressed as a function of the newly defined intermediate variable, z, as

$$u = \frac{-z}{2} - \frac{2 \cdot R \cdot P}{z}, \quad (12)$$

$$\sqrt{u^2 - 4 \cdot P \cdot R} = \frac{z}{2} - \frac{2 \cdot R \cdot P}{z}, \quad (13)$$

$$u + \sqrt{u^2 - 4 \cdot P \cdot R} = \frac{-4 \cdot R \cdot P}{z}. \quad (14)$$

Replacing (12), (13), and (14) in (9) leads to

$$\frac{8 \cdot R^2 \cdot P^2}{z^2} + 2 \cdot R \cdot P - 4 \cdot R \cdot P \cdot ln\left(-\frac{4 \cdot R \cdot P}{z}\right) = h. \quad (15)$$

Equation (15) can be reformulated as

$$\frac{8 \cdot R^2 \cdot P^2}{z^2} - 2 \cdot R \cdot P \cdot ln\left(\frac{16 \cdot R^2 \cdot P^2}{z^2}\right) = h - 2 \cdot R \cdot P. \quad (16)$$

According to the properties of natural logarithms, (16) can be expressed as

$$\frac{8 \cdot R^2 \cdot P^2}{z^2} - 2 \cdot R \cdot P \cdot \left[\ln(2) + ln\left(\frac{8 \cdot R^2 \cdot P^2}{z^2}\right)\right] = h - 2 \cdot R \cdot P. \quad (17)$$

By reassigning the terms in (17), the following equation yields

$$\frac{8 \cdot R^2 \cdot P^2}{z^2} - 2 \cdot R \cdot P \cdot ln\left(\frac{8 \cdot R^2 \cdot P^2}{z^2}\right) = h + 2 \cdot R \cdot P \cdot [\ln(2) - 1]. \quad (18)$$

With the aim turning (18) into a more compact expression, two new intermediate variables are defined at this point,

$$x = \frac{8 \cdot R^2 \cdot P^2}{z^2}, \quad (19)$$

$$g = h + 2 \cdot R \cdot P \cdot [\ln(2) - 1]. \quad (20)$$

Using (19) and (20) in (18) the following expression is obtained,

$$x - 2 \cdot R \cdot P \cdot ln(x) = g. \quad (21)$$

Solving for x in (21) and taking into account the definition of the Lambert W function shown in 3.1 yields

$$x = -2 \cdot R \cdot P \cdot W_{-1}\left(\frac{-\exp\left(\frac{-g}{2 \cdot R \cdot P}\right)}{2 \cdot R \cdot P}\right). \quad (22)$$

By undoing the change of variable in (19), z can now be calculated in closed-form as

$$z = -\sqrt{\frac{4 \cdot R \cdot P}{-W_{-1}\left(\frac{-\exp\left(\frac{-g}{2 \cdot R \cdot P}\right)}{2 \cdot R \cdot P}\right)}}. \quad (23)$$

Note that in (22) and (23), the secondary branch of the Lambert W function has been used. This branch should be taken in the case of a discharge process ($P > 0$). If the SC is charging ($P < 0$), the principal branch must be used. The justification for this will be clarified later. The sign preceding the second term in (23) is selected in order to agree with the physical constraints of the device (u, is always positive). Indeed, according to (11), z should be negative during a discharge process, i.e. $P>0$.

With the aim of simplifying the upcoming expressions a dimensionless function, g_1, is defined as

$$g_1 = -W_{-1}\left(\frac{-\exp\left(\frac{-g}{2 \cdot R \cdot P}\right)}{2 \cdot R \cdot P}\right). \quad (24)$$

Thus, using (24) in (23), z can be expressed as a function of g_1 as

$$z = -\sqrt{\frac{4 \cdot R \cdot P}{g_1}}. \quad (25)$$

3.3. Reformulation of electric variables

Considering (12) and (25), an explicit formulation of the internal voltage of the SC, u, as a function of g_1 can be obtained as follows

$$u = \sqrt{R \cdot P} \cdot \left(\sqrt{g_1} + \frac{1}{\sqrt{g_1}}\right). \quad (26)$$

The rest of the electrical variables involved in the charge/discharge process of the SC can also be easily obtained as a function of g_1, and hence, according to (24), they can be expressed in closed-form as a function of time. For example, the discharge current can be obtained from (3) and (26). The chain rule is needed in that case to obtain the time derivative of the internal voltage,

$$u' = \frac{du}{dg_1} \cdot g_1' = \sqrt{R \cdot P} \cdot \left(\frac{1}{2} \cdot g_1^{-0.5} - \frac{1}{2} \cdot g_1^{-1.5}\right) \cdot g_1'. \quad (27)$$

For its part, the time derivative of g_1 can be easily calculated from (24) as

$$g_1' = -\frac{2}{R \cdot C} \cdot \frac{W_{-1}\left(\frac{-\exp\left(\frac{-g}{2 \cdot R \cdot P}\right)}{2 \cdot R \cdot P}\right)}{1 + W_{-1}\left(\frac{-\exp\left(\frac{-g}{2 \cdot R \cdot P}\right)}{2 \cdot R \cdot P}\right)} = \frac{2}{R \cdot C} \cdot \frac{g_1}{1 - g_1}. \quad (28)$$

Thus, from (3), (27), and (28), the explicit formulation of the discharge current, i, as a function of g_1 can be expressed as

$$i = \sqrt{\frac{P}{R \cdot g_1}}. \quad (29)$$

In the same way, considering the relation between the discharge power and current, P and i, the external voltage of the SC can be expressed in closed-form as

$$u_{co} = \frac{P}{i} = \sqrt{R \cdot P \cdot g_1}. \quad (30)$$

Moreover, SC power losses, p_d, justified in the model by the internal resistance, can be formulated as

$$p_d = R \cdot i^2 = \frac{P}{g_1}. \quad (31)$$

In order to obtain a closed-form of the energy losses, e_d, as a function of g_1, it should be considered that

$$p_d = \frac{de_d}{dt}. \quad (32)$$

By applying the chain rule to (32) and using the result in (31), the following first order differential equation is obtained

$$\frac{P}{g_1} = \frac{de_d}{dg_1} \cdot g_1' = \frac{2}{R \cdot C} \cdot \frac{g_1}{1 - g_1} \cdot \frac{de_d}{dg_1}. \quad (33)$$

The integration of (33) yields to the following closed-form expression of energy losses, where $g_{1(0)}$ stands for the value of g_1 at the initial instant, $t = 0$.

$$e_d = \int_{g_{1(0)}}^{g_1} \frac{R \cdot C \cdot P}{2} \cdot \left(\frac{1 - g_1}{g_1^2}\right) \cdot dg_1 = \frac{R \cdot C \cdot P}{2} \cdot \left[\frac{1}{g_{1(0)}} - \frac{1}{g_1} + ln\left(\frac{g_{1(0)}}{g_1}\right)\right]. \quad (34)$$

Other important variables in the analysis of SCs can be also obtained as a function of g_1. Thus, the following equations show, respectively, closed-form expressions of the instantaneous energy stored in the cell, e_{stored}, the energy discharged since an initial state, e_{dch}, and the state of charge (*SOC*).

$$e_{stored} = \frac{1}{2} \cdot C \cdot u^2 = \frac{R \cdot C \cdot P}{2} \cdot \left(g_1 + \frac{1}{g_1} + 2\right), \quad (35)$$

$$e_{dch} = \frac{1}{2} \cdot C \cdot \left(U_0^2 - u^2\right) = \frac{R \cdot C \cdot P}{2} \cdot \left(\frac{U_0^2}{R \cdot P} - g_1 - \frac{1}{g_1} - 2\right), \quad (36)$$

$$SOC = \frac{e_{stored}}{e_{max}} = \frac{R \cdot P}{U_N^2} \cdot \left(g_1 + \frac{1}{g_1} + 2\right). \quad (37)$$

Notice that in (37), U_N stands for the rated voltage of the SC, wich, for a single cell, is typically within the range 2.7–3 V, and e_{max} is the energy stored at that voltage.

It is important to note that in (22)-(24) and (28) the secondary branch of the Lambert W function, W_{-1}, was selected. In fact, this is the correct choice during a discharge process, i.e. $P>0$. Indeed, under that operating conditions g decreases with time according to (10) and (20) and thus, the same can be said for the argument of the Lambert W function in (24). Considering Fig. 2, the secondary branch of the Lambert W function leads to a positive decreasing value of g_1 while the principal branch leads to a positive increasing value. The first of these alternatives must be selected as, according to (29), the discharge process implies an increasing current and thus, a decreasing value of g_1. On the contrary and for the same reasons, during a charge process, i.e. $P<0$, the principal branch of the Lambert W function, W_0, should be used in (22)-(24) and (28).

From equation (24), an expression yielding time as a function of g_1 can be obtained. According to the properties of the Lambert W function,

$$\frac{-\exp\left(\frac{-g}{2\cdot R\cdot P}\right)}{2\cdot R\cdot P} = -g_1\cdot\exp(-g_1). \tag{38}$$

From the computation of the natural logarithm of both sides of (38),

$$g = 2\cdot R\cdot P\cdot[g_1 - ln(2\cdot R\cdot P\cdot g_1)]. \tag{39}$$

For the sake of simplicity, and from (10) and (20),

$$g = A - \frac{4\cdot P}{C}\cdot t, \tag{40}$$

where A is a constant measured in V^2,

$$A = U_0^2 + U_0\cdot\sqrt{U_0^2 - 4\cdot R\cdot P} - 4\cdot R\cdot P\cdot ln\left(U_0 + \sqrt{U_0^2 - 4\cdot R\cdot P}\right) + 2\cdot R\cdot P\cdot[\ln(2) - 1]. \tag{41}$$

From (39)-(41), time as a function of g_1 can be obtained,

$$t = A_t - \frac{R\cdot C}{2}\cdot(g_1 - ln(2\cdot R\cdot P\cdot g_1)), \tag{42}$$

where A_t is a constant measured in seconds,

$$A_t = \frac{A\cdot C}{4\cdot P}. \tag{43}$$

Once all variables are expressed as a function of g_1, it is interesting to obtain g_1 as a function of them in order to have a set of equations that can be solved for any of the said variables, as well as their respective inverses. Equation (24) already shows g_1 as a function of time. From (29), g_1 can be obtained as a function of the current,

$$g_1 = \frac{P}{R\cdot i^2}. \tag{44}$$

According to the definition of power losses, p_d,

$$g_1 = \frac{P}{p_d}. \tag{45}$$

As shown in (45), g_1 represents the relationship between the charge/discharge power, P, and the power dissipated at the internal resistor, p_d, thus g_1 being dimensionless.

From (30), g_1 can be obtained as a function of the external voltage, u_{co},

$$g_1 = \frac{u_{co}^2}{R\cdot P}. \tag{46}$$

Equation (26) can be solved for g_1 to express the said variable as a function of the internal voltage, u,

$$g_1 = \frac{u}{2\cdot R\cdot P}\cdot\left(u + \sqrt{u^2 - 4\cdot R\cdot P}\right) - 1. \tag{47}$$

From (34), g_1 can be obtained as a function of the energy losses, e_d. Equation (34) can be rewritten as

$$\frac{1}{g_1} - ln\left(\frac{1}{g_1}\right) = \frac{1}{g_{1(0)}} + ln(g_{1(0)}) - \frac{2\cdot e_d}{R\cdot C\cdot P}. \tag{48}$$

Equation (48) can be expressed compactly,

$$\frac{1}{g_1} - ln\left(\frac{1}{g_1}\right) = A_1 - B_1\cdot e_d, \tag{49}$$

by defining two constants,

$$A_1 = \frac{1}{g_{1(0)}} + ln(g_{1(0)}), \tag{50}$$

$$B_1 = \frac{2}{R\cdot C\cdot P}. \tag{51}$$

A_1 being dimensionless, whereas B_1 is measured in J^{-1}. Therefore, from (49),

$$g_1 = \frac{-1}{W_0(-\exp(B_1\cdot e_d - A_1))}. \tag{52}$$

When the variable g_1 is calculated as a function of energy losses, e_d, the principal branch of the Lambert W function must be always taken, independently of the sign of P. Therefore in (52) the $W_0(x)$ form has been used.

Finally, from (35) and (37), g_1 can be expressed as a function of e_{stored}, e_{dch}, and SOC,

$$g_1 = \frac{e_{stored}}{R\cdot C\cdot P} - 1 + \sqrt{\left(\frac{e_{stored}}{R\cdot C\cdot P}\right)^2 - 2\cdot\frac{e_{stored}}{R\cdot C\cdot P}}, \tag{53}$$

$$g_1 = \frac{e_{dch}}{2\cdot R\cdot C\cdot P} - 1 + \sqrt{\left(\frac{e_{dch}}{2\cdot R\cdot C\cdot P}\right)^2 - \frac{e_{dch}}{R\cdot C\cdot P}}, \tag{54}$$

$$g_1 = \frac{U_N^2\cdot SOC}{2\cdot R\cdot P} - 1 + U_N\cdot\sqrt{\left(\frac{U_N\cdot SOC}{2\cdot R\cdot P}\right)^2 - \frac{SOC}{R\cdot P}}. \tag{55}$$

Once all the electrical variables and time are obtained as a function of g_1 and vice versa, any of the said variables can be expressed as a function of the rest of them. For instance (29), and (52) can be combined in order to obtain the current as a function of the energy losses, $i(e_d)$,

Table 1
Electrical parameters of the SC.

U_0 (V)	P(W)	C (kF)	R (mΩ)
2.7	100	1.2	0.58

Table 2
Constants used in case study.

$g_{1(0)}$	A (V^2)	$A_t(s)$	A_1	B_1 (J^{-1})
123.6816	14.0381	42.1143	4.8258	0.0287

$$i(e_d) = \sqrt{-\frac{P}{R} \cdot W_0\left(-\exp(B_1 \cdot e_d - A_1\right)}, \tag{56}$$

and (42), (43), and (45) can be combined to compute how long it takes the power losses, p_d, to reach a specific value,

$$t(p_d) = A_t - \frac{R \cdot C}{2} \cdot \left[\frac{P}{p_d} - ln\left(\frac{2 \cdot R \cdot P^2}{p_d}\right)\right]. \tag{57}$$

As in these examples, the same procedure could be followed to express any variable as a function of the rest.

4. Results and discussion

In this Section, the equations deduced in Section 3 are utilized to obtain all the electrical variables involved in the discharge of a SC whose initial internal voltage, U_0, discharge power, P, and electrical resistance and capacitance, R and C, are known.

A SC discharge process starting from a 2.7-V initial voltage and at a 100-W constant power value during 30 s is studied. The electrical parameters used in this case study are those in Table 1, corresponding to a 1.2 kF cell manufactured by Maxwell Technologies.

Table 2 shows the values of $g_{1(0)}$ ($g_1(t)$ at t = 0), A, A_t, A_1, and B_1, obtained from (24), (41), (43), (50), and (51), respectively.

From the values given in Tables 1 and 2, it is now possible to define the function $g(t)$ with (40). Once $g(t)$ is built, the function

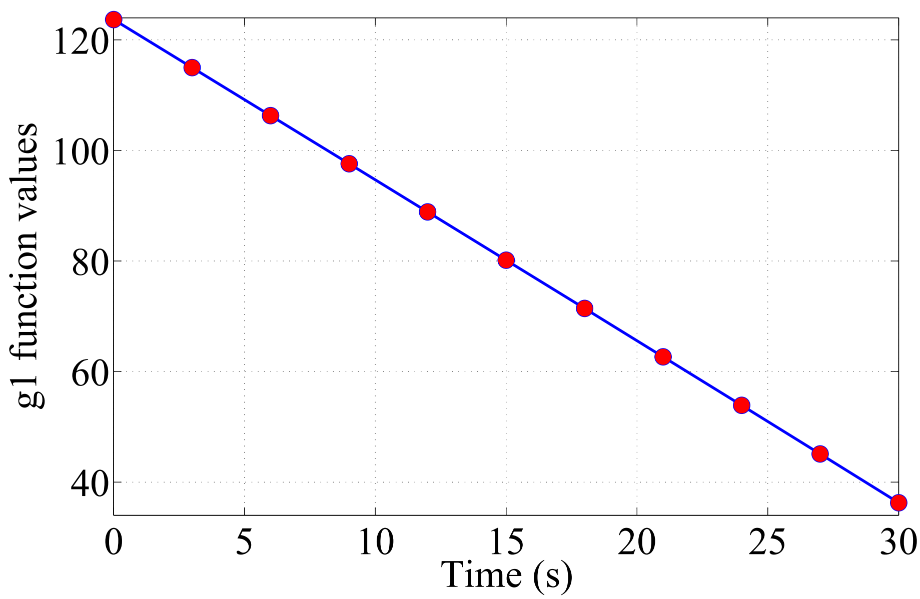

Fig. 3. Values of g_1 as a function of time when using (10), (20) and (24).

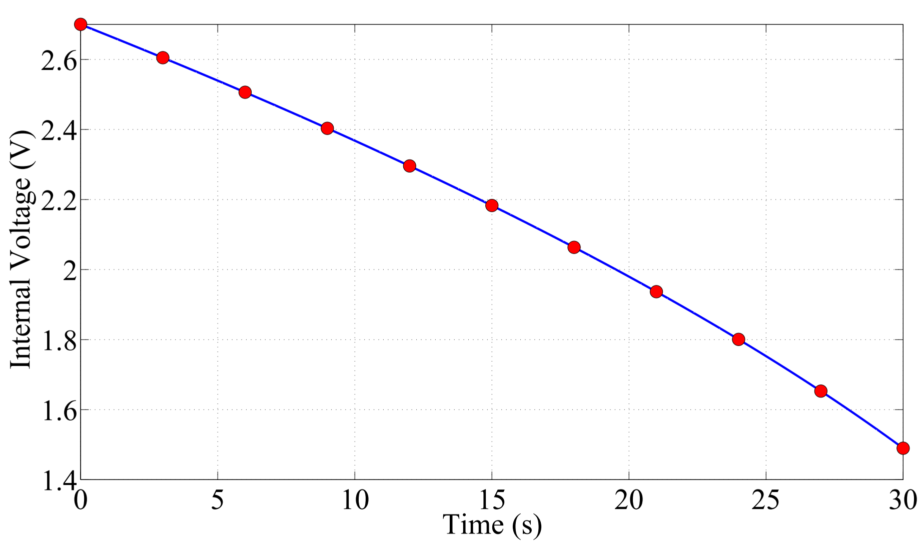

Fig. 4. Internal voltage as a function of time when using (10), (20), (24), and (26).

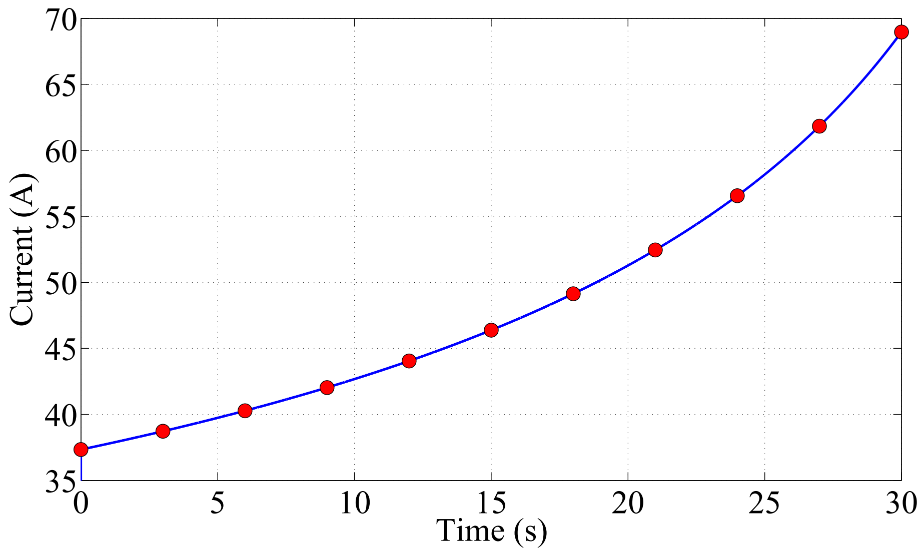

Fig. 5. Current as a function of time when using (10), (20), (24), and (29).

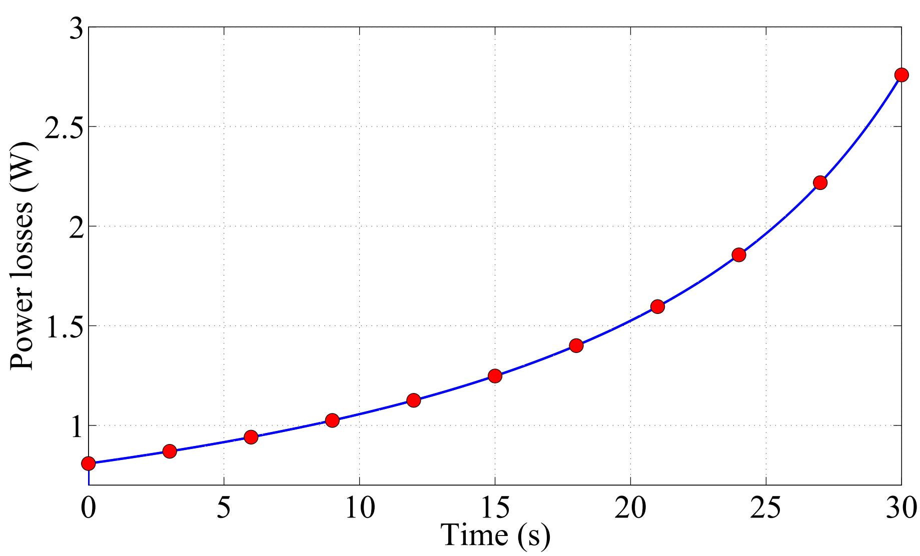

Fig. 6. Power losses as a function of time when using (10), (20), (24), and (31).

$g_1(t)$ will be created with (24). To obtain, the internal voltage, u, the discharge current i, the dissipated power, p_d, and the energy losses e_d, as a function of time, function $g_1(t)$ should be replaced in (26), (29), (31), and (34), respectively. Other electrical variables, such as stored internal energy, e_{stored}, discharged energy, e_{dch}, or the state of charge, SOC, can be obtained using (35), (36), and (37).

Figs. 3–7 show, respectively, the values of g_1, u, i, p_d, and e_d as a function of time, obtained by utilizing the equations proposed in Section 3 for instants taken every 3 s. These results coincide with those that would have been obtained by solving the equations by using numerical methods.

The electrical variables can also be expressed as a function of each other with no need for their being previously computed with respect to time. For instance, Fig. 8 shows the values of $i(e_d)$, i.e. the current as a function of the energy losses, by utilizing (56) straightforwardly, and Fig. 9 shows the values of $p_d(e_d)$, i.e. the power losses as a function of the energy losses, by combining (31) and (52), which yields

$$p_d(e_d) = -P \cdot W_0(-\exp(B_1 \cdot e_d - A_1)) \tag{58}$$

5. Conclusion

In this paper, the Lambert W function is utilized to compute the main electrical variables involved in a SC constant-power charge/discharge cycle. The classical RC-series model is considered and the proposed equations render exact results because no simplifications are made. Therefore, the said results are the same as those obtained when solving the participating differential equations by utilizing numerical methods. However, the proposed strategy is faster than the said numerical methods because all variables can be computed at a given instant from the electrical resistance and capacitance, the

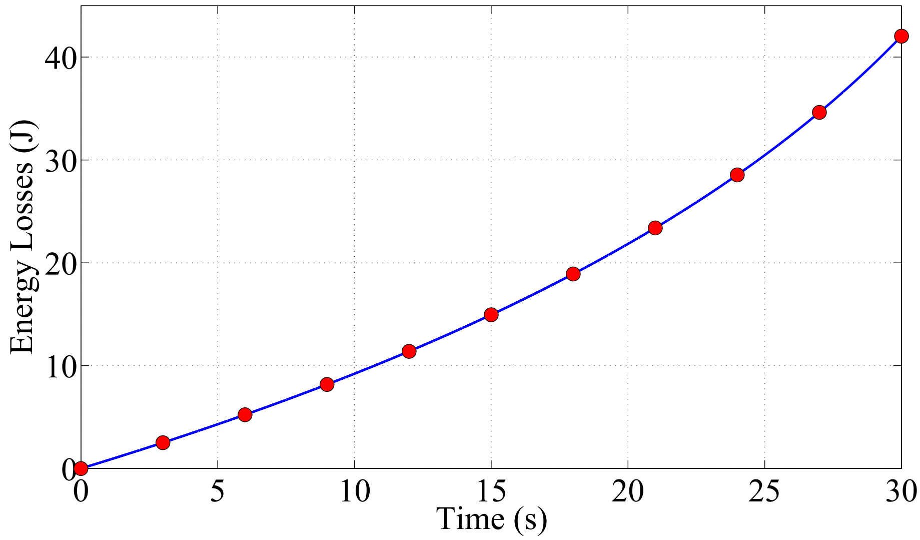

Fig. 7. Energy losses as a function of time when using (10), (20), (24), and (34).

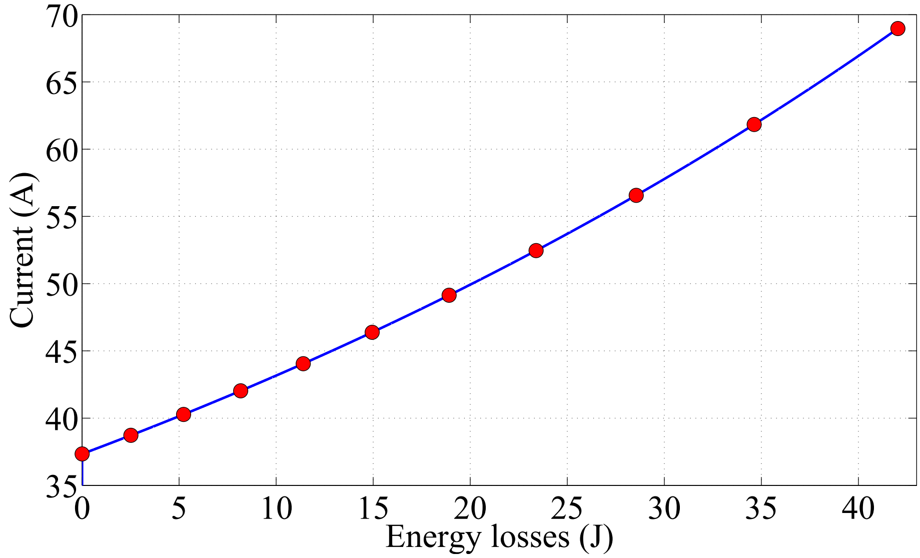

Fig. 8. Current as a function of the energy losses when using (56).

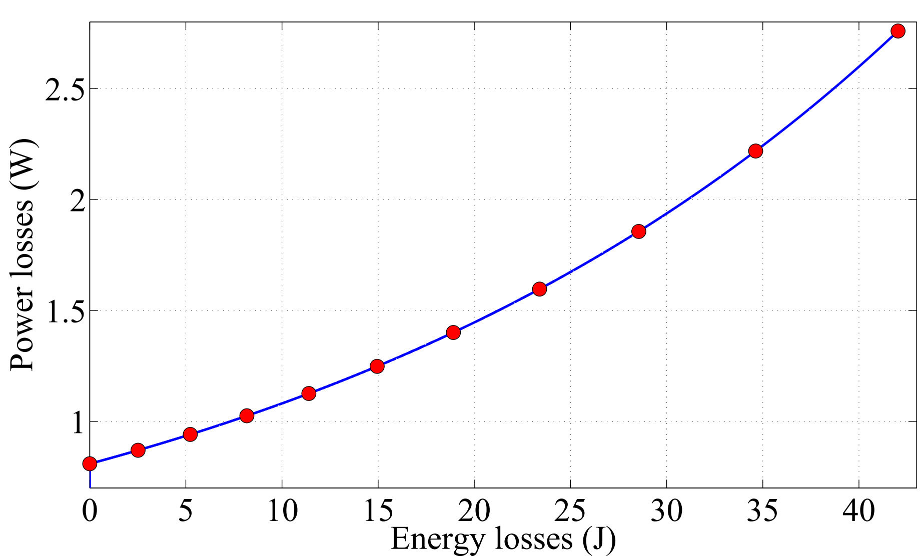

Fig. 9. Power losses as a function of energy losses when using (58).

power, and the initial internal voltage straightforwardly. Any electrical variable involved in the charge/discharge processes can be expressed as a function of time, and as a function of any other electrical variables, by virtue of the proposed formulas. Therefore, a thorough and theoretical basis for developing novel sizing and control techniques for SCs when charged/discharge at constant power is presented.

Author contribution

Joaquín F. Pedrayes: Conceptualization, Methodology, Validation and Writing – original draft Manuel G. Melero: Methodology, Software, Validation and Investigation José M. Cano: Investigation, Data curation, Writing – review & editing, Project administration and Funding acquisition. Joaquín G. Norniella: Supervision, Writing – review & editing: Salvador B. Duque: Software, Validation: Carlos H. Rojas: Software, Validation and Visualization Gonzalo A. Orcajo: Writing – review & editing, Supervision.

Declaration of competing interest

The authors declare that they have no known competing financial interests or personal relationships that could have appeared to influence the work reported in this paper.

Acknowledgements

This work has been funded by the Spanish Government, Innovation Development and Research Office (MEC), under research-grants DPI2017-83804-R, and DPI2017-89186-R.

Appendix A. Supplementary data

Supplementary data to this article can be found online at https://doi.org/10.1016/j.energy.2020.119364.

References

[1] Miller J. Introduction to electrochemical capacitor technology. IEEE Electr Insul Mag Jul. 2010;26(4):40–7.
[2] Kagiri C, Xia X. Optimal control of a hybrid battery/supercapacitor storage for neighborhood electric vehicles. Energy Proc May 2017;105:2145–50.
[3] Kuperman A, Aharon I. Battery-ultracapacitor hybrids for pulsed current loads: a review. Renew Sustain Energy Rev Feb. 2011;15(2):981–92.
[4] Ghenaatian HR, Mousavi MF, Rahmanifar MS. High performance battery-supercapacitor hybrid energy storage system based on self-doped polyaniline nanofibers. Synth Met Sep. 2011;161(17–18). 2017–2023.
[5] Jing W, H Lai C, Wong SHW, Wong MLD. Battery-supercapacitor hybrid energy storage system in standalone DC microgrids: a review. IET Renew Power Gener 2017;11(4). 461-169.
[6] Kim Y, Raghunathan V, Raghunathan A. Design and management of battery-supercapacitor hybrid electrical energy storage systems for regulation services. IEEE Trans Multi-Scale Comput Syst Jan.-Mar. 2017;3(1):12–24.
[7] Lemofouet S, Rufer A. A hybrid energy storage system based on compressed air and supercapacitors with maximum efficiency point tracking (MEPT). IEEE Trans Ind Electron Aug. 2016;53(4):1105–15.
[8] Luta DN, Raji AK. Optimal sizing of hybrid fuel cell-supercapacitor storage system for off-grid renewable applications. Energy Jan. 2019;166(1):530–40.
[9] Kouchachvili L, Yaïci W, Entchev E. Hybrid battery/supercapacitor energy storage system for the electric vehicles. J Power Sources Jan. 2018;374(15):237–48.
[10] Song Z, Hou J, Hofmann H, Li J, Ouyang M. Sliding-mode and Lyapunov function-based control for battery/supercapacitor hybrid energy storage system used in electric vehicles. Energy Mar. 2017;122(1):601–17.
[11] Yu H, Tarsitano D, Hu X, Cheli F. Real time energy management strategy for a fast charging electric urban bus powered by hybrid energy storage system. Energy Oct. 2016;112(1):322–31.
[12] Moreno J, Ortuzar ME, Dixon JW. Energy-management system for a hybrid electric vehicle, using ultracapacitors and neural networks. IEEE Trans Ind Electron 2006;53(2):614–23.
[13] Naseri F, Farjah E, Ghanbari T. An efficient regenerative braking system based on battery/supercapacitor for electric, hybrid, and plug-in hybrid electric vehicles with bldc motor. IEEE Trans Veh Technol 2017;66(5):3724–38.
[14] Abeywardana DBW, Hredzak B, Agelidis VG. A fixed-frequency sliding mode controller for a boost-inverter-based battery-supercapacitor hybrid energy storage system. IEEE Trans Power Electron 2017;32(1):668–80.
[15] Pedrayes JF, Melero MG, Cano JM, Norniella JG, Orcajo GA, Cabanas MF, Rojas CH. Optimization of supercapacitor sizing for high-fluctuating power applications by means of an internal-voltage-based method. Energy Sep. 2019;183:504–13.
[16] Pedrayes J, Melero MG, Norniella JG, Cano JM, Cabanas MF, Orcajo GA, Rojas CH. A novel analytical solution for the calculation of temperature in supercapacitors operating at constant power. Energy Dec. 2019;188:116047.
[17] Zhang L, Hu X, Wang Z, Sun F, Dorrell DG. A review of supercapacitor modeling, estimation, and applications: a control/management perspective. Renew Sustain Energy Rev 2018;81(2):1868–78.
[18] Grbovic PJ, Delarue P, Moigne PL, Bartholomeus P. Modeling and control of the ultracapacitor-based regenerative controlled electric drives. IEEE Trans Ind Electron Aug. 2011;58(8):112–20.
[19] Grbovic PJ. Ultra-capacitors in power conversion systems. IEEE Press Wiley; 2013, ISBN 9781118356265.
[20] Musolino V, Piegari L, Tironi E. New full-frequency-range supercapacitor model with easy identification procedure. IEEE Trans Ind Electron Jan. 2013;60(1):112–20.
[21] Thounthong P, Raël S, Davat B. Analysis of supercapacitor as second source based on fuel cell power generation. IEEE Trans Energy Convers Mar. 2009;24(1):247–55.
[22] Gyawali N, Ohsawa Y. Integrating fuel/electrolyzer/ultracapacitor system into a stand-alone microhydro plant. IEEE Trans Energy Convers Dec. 2010;25(4):1092–101.
[23] Mellincovsky M, Kuperman A, Lerman C, Gadelovits S, Aharon I, Reichbach N, Geula G, Nakash R. Performance and limitations of a constant power-fed supercapacitor. IEEE Trans Energy Convers June 2014;29(2):445–52.
[24] Zhang L, Hu X, Wang Z, Sun F, Deng J, Dorrell DG. Multiobjective optimal sizing of hybrid energy storage system for electric vehicles. IEEE Trans Veh Technol Feb. 2018;67(2):1027–35.
[25] Zhao C, Yin H, Yang Z, Ma C. Equivalent series resistance-based energy loss analysis of a battery semiactive hybrid energy storage system. IEEE Trans Energy Convers Sep. 2015;30(3).
[26] Maxwell Technologies. Datasheet – HC series ultracapacitors. Document #1013793.5.
[27] Maxwell Technologies. Datasheet – K2 series ultracapacitors. Document #1015370.4.
[28] Spyker RL, Nelms RM. Classical equivalent circuit parameters for a double-layer capacitor. IEEE Trans Aero Electron Syst Jul. 2000;36(3):829–36.
[29] Abdel-baqi O, Nasiri A, Miller P. Dynamic performance improvement and peak power limiting using ultracapacitor storage system for hidraulic mining shovels. IEEE IEEE Trans. Ind. Electron. May 2015;62(5):3173–81.
[30] Fouda ME, Allagui A, Elwakil AS, Eltawil A, Kurdahi Fadi. Supercapacitor discharge under constant resistance, constant current and constant power loads. J Power Sources 2019;435:226829.
[31] Miller JM. Ultracapacitor applications. 9781849190718 IET Power and Energy Series 2011;59.
[32] Grbovic PJ, Delarue P, Le Moigne P, Bartholomeus P. The ultracapacitor-based regenerative controlled electric drives with power-smoothing capability. IEEE Trans Ind Electron Dec. 2012;59(12):4511–22.
[33] Gao Q, Zou MY. An analytical solution for two and three dimensional nonlinear Burger's equation. Journal of Applied Mathematical Modelling Dec 2016;45:255–70.
[34] Gómez-Aguilar JF, Martínez HY, Jiménez RFE, Zaragoza CMA, Reyes JR. Analytical and numerical solutions of electrical circuits described by fractional derivatives. Journal of Applied Mathematical Modelling June 2016;40:9079–94.
[35] Gusso A, Pimentel JD. Approximate fully analytical Fourier series solution to the forced and damped Helmholtz-Duffing oscillator. Journal of Applied Mathematical Modelling May 2018;61:593–603.
[36] Basha CA, Rahamathunissa G, Sivakumar S, Lee CW. Numerical and analytical solution of an ODE: strengths and weaknesses of the analytical series solution. Journal of Applied Mathematical Modelling July 2011;36:618–25.
[37] Foyouzat MA, Estekanchi HE, Mofid M. An analytical-numerical solution to assess the dynamic response of viscoelastic plates to a moving mass. Journal of Applied Mathematical Modelling July 2017;54:670–96.
[38] Corless R, Gonnet GH, Hare DEG, Jeffrey DJ, Knuth DE. On the Lambert W function. Adv Comput Math 1996;5:329–59.
[39] Stewart S. Exact answers, old Problems, and a new elementary function. In: Proc. Of the twentieth biennial conference of the Australian association of mathematics; 2005. p. 395–401.